

Dynamics of spiral waves in the complex Ginzburg-Landau equation in bounded domains

M. Aguareles S.J. Chapman T. Witelski

October 1, 2019

Abstract

Multiple spiral wave solutions of the general cubic complex Ginzburg-Landau equation in bounded domains are considered. We investigate the effect of the boundaries on spiral motion under both homogeneous Neumann boundary conditions, for small values of the twist parameter q . We derive explicit laws of motion for rectangular domains and we show that the motion of spirals becomes exponentially slow when the twist parameter exceeds a critical value depending on the size of the domain. The rotational frequency of multispiral patterns is also analytically obtained.

1 Introduction

The complex Ginzburg-Landau equation has a long history in physics as a generic amplitude equation in the vicinity of a Hopf bifurcation in spatially extended systems (see for instance §2 in [12]). It still remains in the forefront of nonlinear science since it is the generic equation for active media displaying plane and rotating wave patterns [4, 11]. The simplest examples of such media are chemical oscillations such as the famous *Belousov-Zhabotinsky* reaction [20]. More complex examples include thermal convection of binary fluids [19], transverse patterns of high intensity light [13]; more recently, it has also been used to model the interaction of several species in some ecological systems [14].

The general cubic complex Ginzburg-Landau equation is given by

$$\frac{\partial \Psi}{\partial t} = \Psi - (1 + ia) |\Psi|^2 \Psi + (1 + ib) \nabla^2 \Psi, \quad (1)$$

where a and b are real parameters and Ψ is a complex field representing the amplitude and phase of the modulations of the oscillatory pattern. The class of solutions that we study in this paper are rotational solutions of (1) with a given frequency ω . In particular, we focus on complex solutions of (1) whose isophase lines have the shape of spiral waves.

Factoring out the rotation and introducing the scalings

$$\Psi = e^{-i\omega t} \sqrt{\frac{1 + \omega b}{1 + ab}} \psi, \quad t = \frac{t'}{1 + \omega b}, \quad (x, y) = \sqrt{\frac{1 + b^2}{1 + b\omega}} (x', y')$$

in (1) gives

$$(1 - ib) \frac{\partial \psi}{\partial t'} = (1 - |\psi|^2) \psi + iq\psi(1 - k^2 - |\psi|^2) + \nabla'^2 \psi, \quad (2)$$

where $q = (a - b)/(1 + ab)$ and k is such that

$$q(1 - k^2) = (\omega - b)(1 + b\omega). \quad (3)$$

The parameters q and k are usually referred to as the *twist parameter* and *asymptotic wavenumber* respectively. When $q = 0$, spiral wave solutions of (2) have isophase lines that are straight lines emanating from some origin (see [10, 17] for more details), while if $q \neq 0$, the isophase lines bend to form spirals. Such complex patterns may be understood in terms of the position of the centres of the spirals, which are often known as *defects*. Thus if the motion of the defects can be determined, much of the dynamics of the solution can be understood.

Of particular interest are spiral wave solutions of (1) in \mathbb{R}^2 . In particular, patterns with a single spiral are topologically stable solutions characterised by the fact that Ψ has a single zero around which the phase of Ψ varies by an integer multiple of 2π that we shall denote as n , which is the winding number of the spiral. Depending on the sign of n the spiral wave unwinds or winds. The time dependence of this type of solution appears as a global rotation, so these solutions are written as $\Psi(\mathbf{x}, t) = e^{-i\omega t}\psi(\mathbf{x})$. Furthermore, $\psi(\mathbf{x})$ has solutions of the form $\psi(\mathbf{x}) = f(r)e^{in\phi+i\chi(r)}$, with r and ϕ the polar radius and azimuthal variables respectively, in which f and χ satisfy a system of ordinary differential equations (see [10] for the derivation and asymptotic properties of these solutions and [15] for a result on existence and uniqueness of solution).

The complex Ginzburg-Landau equation has also more general solutions characterised by a set of zeroes of Ψ from which spirals emanate. Systems with finitely-many zeroes evolve in time in such a way that the spirals preserve their local structure. When the twist parameter vanishes (that is if $a = b$), multispiral solutions in \mathbb{R}^2 move on a time-scale that is proportional to the logarithm of the inverse of the typical spiral separation [16]. As q increases (and so $a \neq b$) the interaction weakens and eventually becomes exponentially small in the separation. When q becomes of order one numerical simulations reveal that the dynamics becomes “frozen”, with a set of virtually independent spirals separated by shock lines [6, 7]. The singular role of the twist parameter, as pointed out in [18], is to interpolate between these two very dissimilar behaviours, namely a strong (algebraic) interaction for small values of q and an exponentially weak interaction as q approaches the critical value of $q_c = \pi/(2 \log d)$, where d is the spiral separation, as is shown in [2, 3].

For a finite set of spirals in the whole of \mathbb{R}^2 , the asymptotic wavenumber k represents the wavenumber of the phase of ψ at infinity that is to say $k = \lim_{t \rightarrow \infty} \arg(\psi)/r$. Therefore, expression (3) represents a dispersion relation, which, when $b = 0$ reads

$$\omega = q(1 - k^2).$$

An important property of spiral wave solutions is that the asymptotic wavenumber k is not a free parameter, but is uniquely determined by q and it is therefore another unknown of the problem. Moreover, k happens to be exponentially small in q which increases the complexity of the problem in the small q limit. In [2, 3], the authors use non-trivial perturbation techniques to derive the asymptotic wavenumber and to obtain laws of motion for the centres of the spirals in the whole of \mathbb{R}^2 .

For ease of exposition we shall take $b = 0$ so that, dropping the primes henceforth, the equation that we shall be considering is

$$\frac{\partial \psi}{\partial t} = \nabla^2 \psi + (1 - |\psi|^2)\psi + iq\psi(1 - k - |\psi|^2). \quad (4)$$

In this paper we focus on multiple-spiral-wave solutions of (4) when the equation is restricted to a bounded domain of \mathbb{R}^2 . We consider homogeneous Neumann (zero flux) boundary conditions; the extension to periodic boundary conditions is easy to make, and together these cover the vast majority of numerical computations and physical applications. We investigate the effect of a bounded domain on the spiral dynamics when the twist parameter is small. An

important motivation of this work is to help elucidate the effect of the boundaries on some features of the dynamics of spirals in order to decide when such interactions are negligible in comparison with the interaction between spirals. We recall that the structural stability of spirals allows us describe the dynamics of spiral wave solutions of (4) in terms of the motion of the centres of the spirals, which are the points at which ψ vanishes. We thus extend our results in [2, 3], where we obtained explicit laws of motion for spirals in free space, and we here derive laws of motion for spirals that are now confined to a bounded domain.

The law of motion we find will be given in terms of the Green's function for a modified Helmholtz equation on Ω , which encodes how the shape of the domain affects the motion of defects. By way of illustration, we then focus on rectangular domains where we obtain explicit laws of motion for a finite set of spirals. As already mentioned, the limit when $q \rightarrow 0$ is highly singular since spiral wave solutions pass from having an algebraic interaction to an exponentially small one. The simulation of the entire system of partial differential equations (1) in this regime is therefore tedious and one usually considers large rectangular domains to simulate spirals in free space. When doing so, one sometimes finds interesting patterns, such as bound states or changes in the direction of interaction of the spirals, which may or may not be due to the effect of the boundaries. Our equations for the motion of spirals in rectangular domains show how much richer their dynamics become in the presence of boundaries. Indeed, one of our main results is to show that what drives the change from an algebraic interaction to an exponentially small motion is in fact how close one gets to a critical relation between the size of the domain and the twist parameter. In particular, we find that the motion of spirals becomes exponentially small when the diameter of the domain approaches $e^{\pi/2q}$, which gives an indication of the difficulty of approximating the solution on an infinite domain with that on a truncated domain.

A second important goal of this paper is to describe the role of the boundaries as a selection mechanism for the rotational frequency ω , and hence for the asymptotic wavenumber k , which we also obtain. In this case we find that as the diameter of the domain approaches $e^{\pi/2q}$, the rotation rate of the patterns also shifts from being algebraic to becoming exponentially small in q .

The paper is organised as follows. Sections §2 and §3 are devoted to obtaining expressions for the laws of motion of the centres of the spirals in general bounded domains. We start in Section §2 by considering what we denote as the *canonical* or *far-field* scale, which corresponds to considering domains of diameter $e^{\pi/2q}$. Then, in Section §3, we consider domains of diameter $\ll e^{\pi/2q}$, which provides a new set of equations for spiral motion in what we denote as the *near field*. In Section §4 we consider the particular case of rectangular domains and we obtain explicit laws of motion in both the far and near field. In particular we find that the interaction between the spirals changes from being exponentially small and mainly in the azimuthal direction when the parameters are in the far field regime to becoming algebraic and with a radial component in the near field. Furthermore, the asymptotic wavenumber and thus the rotational frequency of the patterns is exponentially small in the far-field scaling but proportional to the square root of q and the diameter of the domain in the near field. At the end of Section §4, to reconcile these two regimes, a composite law of motion that is valid in both near and far fields is proposed. This composite law of motion is used to compare the trajectories of the spirals with direct numerical simulations of the whole system of partial differential equations (4). Finally, in Section §5, we present our conclusions.

2 Interaction of spirals in bounded domains at the canonical scale

In this section we derive laws of motion for the centres of a finite set of spirals with unitary winding numbers confined in general bounded domains with homogeneous Neumann boundary conditions. The law of motion and the corresponding asymptotic wavenumber, k , are given explicitly in terms of the parameter q , which is assumed to be small. In what follows we assume that the centres of the spirals are separated from each other and from the boundaries by distances which are large in comparison with the core radius of the spirals. Since in (4) the core radius is $O(1)$, this requires the domain to be large. We quantify this by introducing the inverse of the domain diameter as the small parameter ϵ , and we suppose that spirals are separated by distances of $O(1/\epsilon)$.

We therefore consider the system

$$\begin{aligned} \psi_t &= \psi(1 - |\psi|^2) + iq\psi(1 - k^2 - |\psi|^2) + \nabla^2\psi \quad \text{in } \Omega \\ \frac{\partial\psi}{\partial n} &= 0 \quad \text{on } \partial\Omega, \end{aligned} \tag{5}$$

with parameters $0 < q \ll 1$ and $0 < k \ll 1$. As in unbounded domains (see [2] and [3]), the relationship between ϵ , q and k plays a special role giving place to different types of interaction. In particular, we shall show it is the combination $\alpha = kq/\epsilon$ that determines the nature of the interaction between spirals. In this section we shall assume that α is an order-one constant, and we shall show that this is equivalent to assuming that $1/\epsilon$ is of order $e^{\pi/(2q)}$.

2.1 Outer solution

We follow the same notation as [2] and [3], denoting by $\mathbf{X} = \epsilon\mathbf{x}$ the outer space variable and $T = \mu\epsilon^2t$ the slow time scale on which the spirals to interact. At this stage μ is an unknown small parameter. We will later determine that $\mu = 1/\log(1/\epsilon)$.

Since in this section we are assuming that $\alpha = kq/\epsilon = O(1)$, we write (4) in the outer region as

$$\epsilon^2\mu\psi_T = (1 + iq)\psi(1 - |\psi|^2) - i\frac{\epsilon^2\alpha^2}{q}\psi + \epsilon^2\nabla^2\psi, \quad \text{in } \Omega$$

along with homogeneous Neumann boundary conditions at the domain boundaries, where ∇ now represents the gradient with respect to \mathbf{X} . We express the solution in amplitude-phase form as $\psi = fe^{i\chi}$, giving

$$\mu\epsilon^2 f_T = \epsilon^2\nabla^2 f - \epsilon^2 f|\nabla\chi|^2 + f(1 - f^2), \tag{6}$$

$$\mu\epsilon^2 f^2\chi_T = \epsilon^2\nabla \cdot (f^2\nabla\chi) + qf^2(1 - f^2) - \frac{\epsilon^2\alpha^2}{q}f^2, \tag{7}$$

in Ω , where now the boundary conditions for f and χ are

$$\frac{\partial f}{\partial n} = \frac{\partial\chi}{\partial n} = 0 \quad \text{on } \partial\Omega.$$

Expanding in power series in ϵ^2 as

$$f(\mathbf{X}, T; \epsilon, q) \sim f_0(\mathbf{X}, T; q) + \epsilon^2 f_1(\mathbf{X}, T; q) + \epsilon^4 f_2(\mathbf{X}, T; q) + \dots,$$

$$\chi(\mathbf{X}, T; \epsilon, q) \sim \chi_0(\mathbf{X}, T; q) + \epsilon^2 \chi_1(\mathbf{X}, T; q) + \epsilon^4 \chi_2(\mathbf{X}, T; q) + \dots,$$

the leading and first-order terms in (6) give

$$f_0 = 1, \quad f_1 = -\frac{1}{2}|\nabla\chi_0|^2, \quad (8)$$

Substituting (8) into (7) gives

$$\begin{aligned} \mu \frac{\partial\chi_0}{\partial T} &= \nabla^2\chi_0 + q|\nabla\chi_0|^2 - \frac{\alpha^2}{q} \quad \text{in } \Omega \\ \frac{\partial\chi_0}{\partial n} &= 0 \quad \text{on } \partial\Omega. \end{aligned}$$

We proceed as in [3] and expand χ_0 in terms of the small parameter μ as $\chi_0 \sim \frac{1}{q}(\chi_{00} + \mu\chi_{01} + \dots)$ to find, at leading order,

$$\begin{aligned} 0 &= \nabla^2\chi_{00} + |\nabla\chi_{00}|^2 - \alpha^2 \quad \text{in } \Omega, \\ \frac{\partial\chi_{00}}{\partial n} &= 0 \quad \text{on } \partial\Omega. \end{aligned} \quad (9)$$

Using the Cole-Hopf transformation $\chi_{00} = \log h_0$, equation (9) is transformed into the linear problem

$$\begin{aligned} 0 &= \nabla^2 h_0 - \alpha^2 h_0 \quad \text{in } \Omega, \\ \frac{\partial h_0}{\partial n} &= 0 \quad \text{on } \partial\Omega, \end{aligned} \quad (10)$$

In order to match to a spiral solution locally at near the origin h_0 should have the form $h_0 \sim -\beta \log |\mathbf{X}|$ as $\mathbf{X} \rightarrow \mathbf{0}$ for some constant β [3]. Thus, a solution with N spirals at positions $\mathbf{X}_1, \dots, \mathbf{X}_N$ should satisfy (10) along with

$$h_0 \sim -\beta_j \log |\mathbf{X} - \mathbf{X}_j| \quad \text{as } \mathbf{X} \rightarrow \mathbf{X}_j, \quad \text{for } j = 1, \dots, N. \quad (11)$$

The solution to (10)-(11) is therefore

$$h_0 = -2\pi \sum_{j=1}^N \beta_j G(\mathbf{X}; \mathbf{X}_j) = \mathcal{G}(\mathbf{X}; \alpha(T), \beta_1(T), \dots, \beta_N(T), \mathbf{X}_1(T), \mathbf{X}_2(T), \dots, \mathbf{X}_N(T)), \quad (12)$$

say, where $G(\mathbf{X}; \mathbf{Y})$ is the Neumann Green's function for the modified Helmholtz equation in Ω , satisfying

$$\nabla^2 G - \alpha^2 G = \delta(\mathbf{X} - \mathbf{Y}) \quad \text{in } \Omega, \quad \frac{\partial G}{\partial n} = 0 \quad \text{on } \partial\Omega, \quad (13)$$

and we have been explicit about the dependence of \mathcal{G} on the value of α , the weights β_j , and the position of the spirals \mathbf{X}_j , all of which may depend on T .

2.2 Inner solution

We rescale close to the centre of a spiral \mathbf{X}_ℓ by writing $\mathbf{X} = \mathbf{X}_\ell + \epsilon \mathbf{x}$ to give

$$\begin{aligned} \epsilon \mu \left(\epsilon f_T - \frac{d\mathbf{X}_\ell}{dT} \cdot \nabla f \right) &= \nabla^2 f - f|\nabla\chi|^2 + (1 - f^2)f, \\ \epsilon \mu f^2 \left(\epsilon \chi_T - \frac{d\mathbf{X}_\ell}{dT} \cdot \nabla \chi \right) &= \nabla \cdot (f^2 \nabla \chi) + q(1 - f^2)f^2 - \frac{\epsilon^2 \alpha^2 f^2}{q}, \end{aligned}$$

or equivalently

$$\epsilon\mu \left(\epsilon\psi_T - \frac{d\mathbf{X}_\ell}{dT} \cdot \nabla\psi \right) = \nabla^2\psi + (1+iq)(1-|\psi|^2)\psi - i\frac{\epsilon^2\alpha^2}{q}\psi,$$

where ∇ represents now the gradient with respect to the inner variable \mathbf{x} . Since the inner region does not see the boundary of Ω (since we assume that the distance between the spiral centre and the boundary is much greater than the core radius), the inner equations are to be solved on an unbounded domain, and the same computations presented in [3] hold.

Expanding $f \sim f_0(\mathbf{x}; q, \mu) + \epsilon f_1(\mathbf{x}; q, \mu) + \epsilon^2 f_2(\mathbf{x}; q, \mu) + \dots$ and $\chi \sim \chi_0(\mathbf{x}; q, \mu) + \epsilon \chi_1(\mathbf{x}; q, \mu) + \dots$, or equivalently $\psi \sim \psi_0(\mathbf{x}; q, \mu) + \epsilon \psi_1(\mathbf{x}; q, \mu) + \dots$, the leading-order equation is

$$0 = \nabla^2\psi_0 + (1+iq)\psi_0(1-|\psi_0|^2),$$

with solution $f_0 = f_0(r, T)$ and $\chi_0 = n_\ell\phi + \varphi_0(r, T)$, where r and ϕ are the radial and azimuthal variables with respect to the spiral's centre, $|n_\ell| = 1$ is the spirals' winding number, and f_0 and φ_0 satisfy ordinary differential equations in r which depend on the small parameter q . Expanding further in q as $f_0 \sim f_{00} + f_{01}q + f_{02}q^2 + \dots$ and $\varphi_0 \sim \varphi_{00}/q + \varphi_{01} + \varphi_{02}q + \dots$, gives $\varphi_{00} = \varphi_{00}(T)$, $\varphi_{01} = \varphi_{01}(T)$ and also

$$f_{00}'' + \frac{f_{00}'}{r} - \frac{f_{00}}{r^2} + (1-f_{00}^2)f_{00} = 0, \quad (14)$$

$$\varphi_{02}'(r) = -\frac{1}{rf_{00}^2} \int_0^r s f_{00}^2 (1-f_{00}^2) ds, \quad (15)$$

with boundary conditions $f_{00}(0) = 0$ and $\lim_{r \rightarrow \infty} f_{00}(r) = 1$.

At first order in ϵ it is found

$$-\mu \frac{d\mathbf{X}_\ell}{dT} \cdot \nabla\psi_0 = \nabla^2\psi_1 + (1+iq)(\psi_1(1-2|\psi_0|^2) - \psi_0^2\psi_1^*), \quad (16)$$

or equivalently, in terms of f_1 and χ_1 ,

$$-\mu \frac{d\mathbf{X}_\ell}{dT} \cdot \nabla f_0 = \nabla^2 f_1 - f_1 |\nabla \chi_0|^2 - 2f_0 \nabla \chi_0 \cdot \nabla \chi_1 + f_1 - 3f_0^2 f_1, \quad (17)$$

$$-\mu f_0^2 \frac{d\mathbf{X}_\ell}{dT} \cdot \nabla \chi_0 = \nabla \cdot (f_0^2 \nabla \chi_1) + \nabla \cdot (2f_0 f_1 \nabla \chi_0) + 2q f_0 f_1 - 4q f_0^3 f_1. \quad (18)$$

2.3 Inner limit of the outer

We define the regular part of the outer solution \mathcal{G} near the ℓ th spiral by setting

$$\mathcal{G}_{\text{reg}}^\ell(\mathbf{X}) = \mathcal{G}(\mathbf{X}) + \beta_\ell \log |\mathbf{X} - \mathbf{X}_\ell(T)|.$$

Then, from (12), as \mathbf{X} approaches \mathbf{X}_ℓ , we find

$$h_0 \sim -\beta_\ell \log |\mathbf{X} - \mathbf{X}_\ell| + \mathcal{G}_{\text{reg}}^\ell(\mathbf{X}_\ell) + (\mathbf{X} - \mathbf{X}_\ell) \cdot \nabla \mathcal{G}_{\text{reg}}^\ell(\mathbf{X}_\ell) + \dots$$

Thus, written in terms of the inner variables,

$$\chi_0 \sim \frac{1}{q} \log h_0 \sim \frac{1}{q} \log \left(-\beta_\ell \log(\epsilon r) + \mathcal{G}_{\text{reg}}^\ell(\mathbf{X}_\ell) \right) + \frac{\epsilon \mathbf{x} \cdot \nabla \mathcal{G}_{\text{reg}}^\ell(\mathbf{X}_\ell)}{q (-\beta_\ell \log(\epsilon r) + \mathcal{G}_{\text{reg}}^\ell(\mathbf{X}_\ell))} + \dots, \quad (19)$$

where $r = R/\epsilon = |\mathbf{X} - \mathbf{X}_\ell(T)|/\epsilon$.

2.4 Outer limit of the inner

Using (15) along with the fact that $f_{00} \sim 1 - 1/r^2$ as $r \rightarrow \infty$, it is found that

$$\frac{\partial \varphi_{02}}{\partial r} \sim -q \frac{\log r + c_1}{r} + \dots, \quad (20)$$

as $r \rightarrow \infty$, where c_1 is a constant given by

$$c_1 = \lim_{r \rightarrow \infty} \left(\int_0^r f_0^2(s) (1 - f_0(s)^2) s \, ds - \log(r) \right).$$

However, in order to match with the outer expansion we need the outer limit of the whole expansion in q . This can be found to be of the form

$$f_0 \sim 1 + \frac{1}{r^2} \sum_{i=0}^N C_i (q(\log(r) + c_1))^{2i} + \dots, \quad (21)$$

$$\frac{\partial \chi_0}{\partial r} \sim -\frac{1}{r} \sum_{i=0}^N D_i (q(\log(r) + c_1))^{2i+1} + \dots, \quad (22)$$

where $C_i > 0$ and $D_i > 0$ are constant values independent of q . The necessity of taking all the terms in q when matching can be seen, since the expansion in q is valid only when $q(\log(r) + c_1) \ll 1$. When $\alpha = O(1)$, q turns out to be $O(1/\log \epsilon)$ and thus all the terms in (21)-(22) are the same order. We can sum all these terms in the outer limit of the inner expansion using the same method as in Section 3.3.1 in [3]. The idea is to rewrite the leading-order inner equations in terms of the outer variable $R = \epsilon r$ to obtain

$$0 = \epsilon^2 (\nabla^2 f_0 - f_0 |\nabla \chi_0|^2) + (1 - f_0^2) f_0, \quad (23)$$

$$0 = \epsilon^2 \nabla \cdot (f_0^2 \nabla \chi_0) + q(1 - f_0^2) f_0^2. \quad (24)$$

We now expand in powers of ϵ as $\chi_0 \sim \widehat{\chi}_{00}(r, \phi; q) + \epsilon^2 \widehat{\chi}_{01}(r, \phi; q) + \dots$ and $f_0 \sim \widehat{f}_{00}(r, \phi; q) + \epsilon^2 \widehat{f}_{01}(r, \phi; q) + \dots$. The leading-order term in this expansion $\widehat{\chi}_{00}(r, \phi; q)$ is just the first term (in ϵ) in the outer expansion of the leading-order inner solution, including all the terms in q . Substituting these expansions into (23), (24) gives $\widehat{f}_{00} = 1$, $\widehat{f}_{01} = -\frac{1}{2} |\nabla \widehat{\chi}_{00}|^2$ and

$$0 = \nabla^2 \widehat{\chi}_{00} + q |\nabla \widehat{\chi}_{00}|^2,$$

that is a Riccati equation which can be linearised with the change of variable $\widehat{\chi}_{00} = (1/q) \log \widehat{h}_0$ to give $\nabla^2 \widehat{h}_0 = 0$.

Since $\widehat{\chi}_{00} = n_\ell \phi + \widehat{\varphi}(R)$ we set $\widehat{h}_0 = e^{qn_\ell \phi} e^{q\widehat{\varphi}(R)} = e^{qn_\ell \phi} H_0(R)$ to give

$$H_0'' + \frac{H_0'}{R} + q^2 \frac{H_0}{R^2} = 0,$$

with solution

$$H_0 = A_\ell(q) \epsilon^{-iqn_\ell} R^{iqn_\ell} + B_\ell(q) \epsilon^{iqn_\ell} R^{-iqn_\ell}, \quad (25)$$

where A_ℓ and B_ℓ are constants that depend on q which may be different at each vortex, and the factors $\epsilon^{\pm iqn_\ell}$ are included to facilitate their determination by comparison with the solution in the inner variable. To determine A_ℓ and B_ℓ we need to write $\widehat{\chi}_{00}$ in terms of r , expand in powers of q , and compare with (20). Writing the constants in powers of q as $A_\ell(q) \sim$

$A_{\ell 0}/q + A_{\ell 1} + qA_{\ell 2} + \dots$ and $B_{\ell}(q) \sim B_{\ell 0}/q + B_{\ell 1} + qB_{\ell 2} + \dots$, and expressing H_0 in terms of r we find

$$\begin{aligned} H_0(r) &= A_{\ell}(q)e^{iqn_{\ell} \log r} + B_{\ell}(q)e^{-iqn_{\ell} \log r} \\ &\sim \frac{A_{\ell 0} + B_{\ell 0}}{q} + A_{\ell 1} + B_{\ell 1} + (A_{\ell 0} - B_{\ell 0})in_{\ell} \log r \\ &\quad + q \left(A_{\ell 2} + B_{\ell 2} + (A_{\ell 1} - B_{\ell 1})in_{\ell} \log r - \frac{(A_{\ell 0} + B_{\ell 0})}{2} \log^2 r \right) + \dots, \end{aligned}$$

so that

$$\begin{aligned} \frac{\partial \widehat{\chi}_{00}}{\partial r} &= \frac{H'_0(r)}{qH_0(r)} \sim \frac{n_{\ell}(A_{\ell 0} - B_{\ell 0})i}{r(A_{\ell 0} + B_{\ell 0})} + q \left(\frac{(A_{\ell 1} - B_{\ell 1})}{(A_{\ell 0} + B_{\ell 0})} \frac{n_{\ell}i}{r} - \frac{\log r}{r} \right. \\ &\quad \left. + \frac{(A_{\ell 0} - B_{\ell 0})^2 \log r}{(A_{\ell 0} + B_{\ell 0})^2} \frac{1}{r} - \left(\frac{i(A_{\ell 0} - B_{\ell 0})(A_{\ell 1} + B_{\ell 1})}{(A_{\ell 0} + B_{\ell 0})^2} \right) \frac{n_{\ell}}{r} \right) + \dots \end{aligned}$$

Comparing with (20) (and recalling that $n_{\ell} = \pm 1$) we see that

$$A_{\ell 0} - B_{\ell 0} = 0, \quad (26)$$

$$\frac{(A_{\ell 1} - B_{\ell 1})}{A_{\ell 0} + B_{\ell 0}}i = -n_{\ell}c_1 \quad \text{for } \ell = 1, \dots, N. \quad (27)$$

The remaining equations determining A_{ℓ} and B_{ℓ} will be fixed when matching with the outer region.

Outer limit of the first-order inner We do the same with the first-order inner solution. The details of the calculations, which we summarize in what follows, are the same as in Section 4.3.4 in [3]. We first write equation (17)-(18) in terms of the outer variable to give

$$\begin{aligned} -\epsilon\mu \frac{d\mathbf{X}_{\ell}}{dT} \cdot \nabla f_0 &= \epsilon^2 \nabla^2 f_1 - \epsilon^2 f_1 |\nabla \chi_0|^2 - 2\epsilon^2 f_0 \nabla \chi_0 \cdot \nabla \chi_1 + f_1 - 3f_0^2 f_1, \\ -\mu \epsilon f_0^2 \frac{d\mathbf{X}_{\ell}}{dT} \cdot \nabla \chi_0 &= \epsilon^2 \nabla \cdot (f_0^2 \nabla \chi_1) + \epsilon^2 \nabla \cdot (2f_0 f_1 \nabla \chi_0) + 2qf_0 f_1 - 4qf_0^3 f_1. \end{aligned}$$

We now expand in powers of ϵ as $\chi_1 \sim \widehat{\chi}_{10}(q)/\epsilon + \widehat{\chi}_{11}(q) + \dots$ and $f_1 \sim \widehat{f}_{10}(q) + \epsilon \widehat{f}_{11}(q) + \dots$ to give $\widehat{f}_{10} = 0$, $\widehat{f}_{11} = -\nabla \widehat{\chi}_{00} \cdot \nabla \widehat{\chi}_{10}$ and

$$-\mu \frac{d\mathbf{X}_{\ell}}{dT} \cdot \nabla \widehat{\chi}_{00} = \nabla^2 \widehat{\chi}_{10} + 2q \nabla \widehat{\chi}_{00} \cdot \nabla \widehat{\chi}_{10}. \quad (28)$$

Motivated by the transformation we applied to $\widehat{\chi}_{00}$ we write $\widehat{\chi}_{10} = \widehat{h}_1 / (q\widehat{h}_0) = \widehat{h}_1 e^{-q\widehat{\chi}_{00}} / q$ and (28) becomes

$$-\mu \frac{d\mathbf{X}_{\ell}}{dT} \cdot \nabla \widehat{\chi}_{00} = \frac{e^{-q\widehat{\chi}_{00}}}{q} \nabla^2 \widehat{h}_1.$$

Writing $\widehat{\chi}_{00}$ in terms of \widehat{h}_0 gives

$$-\mu \frac{d\mathbf{X}_{\ell}}{dT} \cdot \nabla \widehat{h}_0 = \nabla^2 \widehat{h}_1. \quad (29)$$

Writing the velocity as

$$\frac{d\mathbf{X}_{\ell}}{dT} = (V_1, V_2)$$

and recalling that $\widehat{h}_0 = e^{qn_\ell\phi} H_0(R)$, the left hand side of (29) gives

$$\begin{aligned} -\mu \frac{d\mathbf{X}_\ell}{dT} \cdot \left(\frac{qn_\ell e^{qn_\ell\phi} H_0(R)}{R} \mathbf{e}_\theta + H'_0(R) e^{qn_\ell\phi} \mathbf{e}_R \right) \\ = -\frac{\mu q n_\ell e^{qn_\ell\phi}}{R} \left(e^{i\phi} R^{iqn_\ell} A_\ell \epsilon^{-iqn_\ell} (V_2 + iV_1) - e^{-i\phi} R^{-iqn_\ell} B_\ell \epsilon^{iqn_\ell} (V_2 - iV_1) \right), \end{aligned}$$

since

$$\begin{aligned} \frac{H_0(R)}{R} &= A_\ell(q) \epsilon^{-iqn_\ell} R^{iqn_\ell-1} + B_\ell(q) \epsilon^{iqn_\ell} R^{-iqn_\ell-1}, \\ H'_0(R) &= iqn_\ell A_\ell(q) \epsilon^{-iqn_\ell} R^{iqn_\ell-1} - iqn_\ell B_\ell(q) \epsilon^{iqn_\ell} R^{-iqn_\ell-1}. \end{aligned}$$

Therefore, writing

$$\widehat{h}_1 = -\mu q n_\ell A_\ell \epsilon^{-iqn_\ell} (V_2 + iV_1) g_1(R) e^{(qn_\ell+i)\phi} - \mu q n_\ell B_\ell \epsilon^{iqn_\ell} (V_2 - iV_1) g_2(R) e^{(qn_\ell-i)\phi},$$

yields a system of equations for g_1 and g_2 , whose solution gives

$$\begin{aligned} \widehat{h}_1 &= -\frac{\mu A_\ell \epsilon^{-iqn_\ell} (V_1 - iV_2)}{4} (R^{iqn_\ell+1} + \gamma_1 R^{1-iqn_\ell}) e^{(qn_\ell+i)\phi} \\ &\quad - \frac{\mu B_\ell \epsilon^{iqn_\ell} (V_1 + iV_2)}{4} (R^{-iqn_\ell+1} + \gamma_2 R^{1+iqn_\ell}) e^{(qn_\ell-i)\phi}. \end{aligned} \quad (30)$$

where γ_1 and γ_2 are unknown constants that will be determined by matching to the inner limit of the outer solution.

2.5 Leading order matching: determination of the asymptotic wavenumber

Using (25) and (26), the leading-order outer limit of the inner expansion is found to be,

$$\widehat{\chi}_{00} \sim \frac{1}{q} \log H_0 + O(1) \sim \frac{1}{q} \log \left(\frac{A_{0\ell} e^{-iqn_\ell \log \epsilon} + A_{0\ell} e^{iqn_\ell \log \epsilon}}{q} + O(1) \right),$$

while the leading-order inner limit of the outer, according to (19) reads

$$\chi_{00} \sim \frac{1}{q} \log \left(-\beta_\ell \log(\epsilon r) + \mathcal{G}_{\text{reg}}^\ell(\mathbf{X}_\ell) + O(\epsilon r) \right). \quad (31)$$

Hence, in order to match, the order $1/q$ term inside the logarithm in the outer limit of the inner must vanish, so that

$$e^{-iqn_\ell \log \epsilon} + e^{iqn_\ell \log \epsilon} = O(q) \quad \text{or equivalently} \quad q |\log \epsilon| = \frac{\pi}{2} + q\nu, \quad (32)$$

where ν is an order one constant and $|n_\ell| = 1$. This expression provides a relation between the two small parameters q and ϵ , and it is needed in order for α to be an order one constant. It is equivalent to assuming that the typical size domain is $1/\epsilon = O(e^{\pi/2q})$.

The outer limit of the inner now reads

$$\widehat{\chi}_{00} \sim \frac{1}{q} \log (-2A_{0\ell}\nu + in_\ell(A_{1\ell} - B_{1\ell}) - 2A_{0\ell} \log R + \dots),$$

and matching with (31) provides the conditions $A_{0\ell} = \beta_\ell/2$ and

$$\mathcal{G}_{\text{reg}}^\ell(\mathbf{X}_\ell) = -2A_{0\ell}\nu + in_\ell(A_{1\ell} - B_{1\ell}).$$

Eliminating $A_{1\ell} - B_{1\ell}$ using (27) gives

$$\mathcal{G}_{\text{reg}}^\ell(\mathbf{X}_\ell) + \beta_\ell(c_1 + \nu) = 0. \quad (33)$$

With ν given by (32), this provides a set of N equations for the $N + 1$ unknowns α and β_ℓ , $\ell = 1, \dots, N$. However, since $\mathcal{G}_{\text{reg}}^\ell(\mathbf{X}_\ell)$ is a homogeneous, linear function of β_1, \dots, β_N (see (12)), the system (33) is a homogeneous linear system of N equations for β_1, \dots, β_N . There exists a solution if and only if the determinant of the system is zero, which provides an equation for α . This in turn determines the asymptotic wavenumber, $k = \alpha\epsilon/q$, and therefore the rotational frequency ω . The coefficients β_1, \dots, β_N are then determined only up to some global scaling (which is equivalent to adding a constant to χ_{00}).

2.6 First order matching: law of motion for the centres of the spirals

We now compare one term of the outer expansion with two terms of the inner expansion (in the notation of Van Dyke [9]). This matching will eventually provide a law of motion for the spirals.

The two-term inner expansion of the one-term outer solution for χ is given in (19). We must compare this with the one-term outer expansion of the two-term inner solution $\chi_0 + \epsilon\chi_1$. From §2.4 the one-term (in ϵ) outer expansion of this is

$$\frac{1}{q} \log(\widehat{h}_0) + \frac{\widehat{h}_1}{q\widehat{h}_0}. \quad (34)$$

Comparing this with (19) gives the matching condition

$$\mathbf{x} \cdot \nabla \mathcal{G}_{\text{reg}}^\ell(\mathbf{X}_\ell) = \frac{\mu r i n_\ell A_{0\ell}}{4q} \left(e^{i\phi}(V_1 - iV_2)(1 + \gamma_1) - e^{-i\phi}(V_1 + iV_2)(1 + \gamma_2) \right).$$

Note that this equation implies that $\mu = O(q)$, as we have been supposing. Solving for γ_1 and γ_2 , substituting into (30), writing $\widehat{\chi}_{10}$ in terms of the inner variable and expanding in powers of q finally gives, to leading order in q ,

$$\chi_{10} \sim -\frac{\mu r}{2q}(V_1 \cos \phi + V_2 \sin \phi) + \frac{n_\ell r}{\beta_\ell} \nabla \mathcal{G}_{\text{reg}}^\ell(\mathbf{X}_\ell) \cdot \mathbf{e}_\phi \quad \text{as } r \rightarrow \infty. \quad (35)$$

Solvability condition and law of motion Equation (35) provides a boundary condition on the first-order inner equation (16). However, there is a solvability condition on (16) subject to (35), which determines V_1 and V_2 , thereby providing our law of motion for the spiral centres. The analysis in this section summarises the corresponding analysis in [3].

Multiplying equation (16) by the conjugate v^* of a solution v of the adjoint problem

$$\nabla^2 v + (1 - iq)(v(1 - 2|\psi_0|^2) - \psi_0^2 v^*) = 0,$$

integrating over a ball B_{r^*} of radius r^* , and using integration by parts gives, after some manipulation,

$$-\int_{B_{r^*}} \Re \left\{ (1 - iq) \mu v^* \frac{d\mathbf{X}_\ell}{dT} \cdot \nabla \psi_0 \right\} dS = \int_{\partial B_{r^*}} \Re \left\{ (1 - iq) \left(v^* \frac{\partial \psi_1}{\partial n} - \frac{\partial v^*}{\partial n} \psi_1 \right) \right\} ds, \quad (36)$$

where \Re denotes the real part. A straightforward calculation shows that directional derivatives of ψ_0 are solutions of the adjoint problem if q is replaced by $-q$, i.e. $v = \mathbf{d} \cdot \nabla \psi_0|_{q \rightarrow -q}$, where \mathbf{d} is any vector in \mathbb{R}^2 . To leading order in q and μ the solvability condition (36) is

$$0 = \int_{\partial B_{r^*}} \Re \left\{ (\mathbf{d} \cdot \nabla \psi_0^*) \frac{\partial \psi_1}{\partial n} - \frac{\partial (\mathbf{d} \cdot \nabla \psi_0^*)}{\partial n} \psi_1 \right\} ds.$$

Letting the ball radius r^* tend to infinity gives

$$\lim_{r \rightarrow \infty} \int_0^{2\pi} (\mathbf{e}_\phi \cdot \mathbf{d}) \left(\frac{\partial \chi_{10}}{\partial r} + \frac{\chi_{10}}{r} \right) d\phi = 0. \quad (37)$$

Now using (35) gives the law of motion

$$\frac{d\mathbf{X}_\ell}{dT} = -\frac{2qn_\ell}{\beta_\ell\mu} \nabla^\perp \mathcal{G}_{\text{reg}}^\ell(\mathbf{X}_\ell) + O(q), \quad (38)$$

where $^\perp$ represents a positive rotation by $\pi/2$.

Summary The parameter α and the coefficients β_j are determined (up to a scaling) by the linear system (33), which is

$$2\pi\beta_\ell G_{\text{reg}}(\mathbf{X}_\ell; \mathbf{X}_\ell) + 2\pi \sum_{j=1, j \neq \ell}^N \beta_j G(\mathbf{X}_\ell; \mathbf{X}_j) - \beta_\ell(c_1 + \nu) = 0, \quad (39)$$

where

$$G_{\text{reg}}(\mathbf{X}; \mathbf{Y}) = G(\mathbf{X}; \mathbf{Y}) - \frac{1}{2\pi} \log |\mathbf{X} - \mathbf{Y}|,$$

is the regular part of the Neumann Green's function G for the modified Helmholtz equation (13), and $\nu = \log(1/\epsilon) - \pi/2q$. The law of motion (38) may be written, to leading order in q , as

$$\frac{d\mathbf{X}_\ell}{dT} = \frac{4\pi q n_\ell}{\beta_\ell \mu} \sum_{j=1, j \neq \ell}^N \beta_j \nabla^\perp G(\mathbf{X}_\ell; \mathbf{X}_j) + \frac{4\pi q n_\ell}{\mu} \nabla^\perp G_{\text{reg}}(\mathbf{X}_\ell; \mathbf{X}_\ell) \quad (40)$$

As the size of the domain tends to infinity,

$$G(\mathbf{X}; \mathbf{Y}) \rightarrow -\frac{1}{2\pi} K_0(\alpha |\mathbf{X} - \mathbf{Y}|), \quad (41)$$

and equation (40) agrees with that given in [2] for spirals in an infinite domain.

3 Interaction of spirals in bounded domains in the near-field

In the previous section we assumed the parameter α is order one as $\epsilon \rightarrow 0$, which led to q and ϵ being related by (32), which implies that the separation of spirals, and therefore the size of the domain, is exponentially large in q .

We now consider smaller domains, in which α will be small. We will find that $\alpha = O(q^{1/2})$ in this new scale in contrast to spirals in the near field in the whole of \mathbb{R}^2 , where α is found to be exponentially small in q [2].

3.1 Outer region

As before we rescale time as $T = \mu\epsilon^2 t$ and use $\mathbf{X} = \epsilon\mathbf{x}$ as the outer variable, to give

$$\epsilon^2 \mu \psi_T = (1 + iq) \psi(1 - |\psi|^2) - i \frac{\epsilon^2 \alpha^2}{q} \psi + \epsilon^2 \nabla^2 \psi \quad \text{in } \Omega.$$

Recall that $1/\epsilon$ is the typical domain diameter in \mathbf{x} , so that the diameter of the domain is $O(1)$ in terms of \mathbf{X} . Expressing the solution in amplitude-phase form as $\psi = fe^{i\chi}$ yields

$$\mu\epsilon^2 f_T = \epsilon^2 \nabla^2 f - \epsilon^2 f |\nabla \chi|^2 + f(1 - f^2), \quad (42)$$

$$\mu\epsilon^2 f^2 \chi_T = \epsilon^2 \nabla \cdot (f^2 \nabla \chi) + qf^2(1 - f^2) - \frac{\epsilon^2 \alpha^2}{q} f^2, \quad (43)$$

in Ω , where, as before, the boundary conditions for f and χ are

$$\frac{\partial f}{\partial n} = \frac{\partial \chi}{\partial n} = 0 \quad \text{on} \quad \partial\Omega.$$

Expanding in asymptotic power series in ϵ as $f \sim f_0 + \epsilon^2 f_1 + \dots$ and $\chi \sim \chi_0 + \epsilon^2 \chi_1 + \dots$, the leading- and first-order terms in f give

$$f_0 = 1, \quad f_1 = -\frac{1}{2} |\nabla \chi_0|^2.$$

The equation for the leading-order phase function, χ_0 , is

$$\begin{aligned} \mu \frac{\partial \chi_0}{\partial T} &= \nabla^2 \chi_0 + q |\nabla \chi_0|^2 - \frac{\alpha^2}{q} \quad \text{in} \quad \Omega, \\ \frac{\partial \chi_0}{\partial n} &= 0 \quad \text{on} \quad \partial\Omega. \end{aligned}$$

So far the analysis is exactly the same as before. However, we know that α cannot be $O(1)$ this time, and so must be some lower order in q . The natural assumption is that $\alpha^2 = O(q)$, which we will verify a posteriori. We thus rescale $\alpha = q^{1/2} \bar{\alpha}$. We note that α being of order $q^{1/2}$ is consistent with the value of α that is found in [1] for a single spiral in a finite disk with homogeneous Neumann boundary conditions.

Expanding χ_0 in terms of q as $\chi_0 \sim \frac{1}{q}(\chi_{00} + q\chi_{01} + \dots)$ as in §2¹ gives, at leading and first order in q ,

$$0 = \nabla^2 \chi_{00} + |\nabla \chi_{00}|^2, \quad (44)$$

$$\tilde{\mu} \frac{\partial \chi_{00}}{\partial T} = \nabla^2 \chi_{01} + 2\nabla \chi_{00} \cdot \nabla \chi_{01} - \bar{\alpha}^2, \quad (45)$$

in Ω , with homogeneous Neumann boundary conditions, where $\tilde{\mu} = \mu/q$. Integrating (44) over Ω and using the divergence theorem and the boundary conditions gives

$$\int_{\Omega} |\nabla \chi_{00}|^2 dS = 0,$$

so that in fact $\chi_{00} = C_1(T)$. Now (42)-(43) are invariant with respect to the transformation

$$\chi \rightarrow \chi - C_1(T)/q, \quad \alpha^2 \rightarrow \alpha^2 + \mu C_1'(T),$$

so that we may take $C_1 \equiv 0$ without loss of generality. In fact, if $C_1'(T) \neq 0$ it means we have not factored out all the bulk rotation when making the change of variables which leads to (2). However, we must be careful when matching with the inner region near each spiral, since changing C_1 is equivalent to scaling A_ℓ in the inner region. With $C_1 = 0$ we will find that the inner expansions for A_ℓ and B_ℓ start at $O(1)$ rather than $O(1/q)$ as they did in §2.4.

¹Note that in §2 we expanded in μ rather than q . The two expansions are equivalent since $\mu = O(q)$, but it is more natural given we will find $\nabla \chi_{00} = 0$ to expand in q in the present case.

The first-order equation (45) becomes

$$\begin{aligned}\nabla^2 \chi_{01} &= \bar{\alpha}^2, & \text{in } \Omega, \\ \frac{\partial \chi_{01}}{\partial n} &= 0 & \text{on } \partial\Omega, \\ \chi_{01} &\sim C_{2j}(T) \log R_j + n_j \phi_j, & \text{as } R_j \rightarrow 0, \quad \text{for } j = 1, \dots, N,\end{aligned}\tag{46}$$

where $R_j = |\mathbf{X} - \mathbf{X}_j(T)|$ and ϕ_j are polar coordinates centred on the j th spiral, and we have assumed that the singularities due to the spirals are locally of the same form as the corresponding singularities when $\Omega = \mathbb{R}^2$ [2]. We thus have a set of unknown slow-time-dependent parameters, $C_{2j}(T)$, one for each spiral, which are determined by matching at each spiral core.

To determine $\bar{\alpha}$ we integrate equation (46) over the domain $V_\delta = \Omega \setminus \sum_{j=1}^N B_\delta(\mathbf{X}_j(T))$, which is the domain that is left after removing disks of radius δ centred at each spiral. Applying the Divergence Theorem on this domain (on which solutions are regular), and then taking the limit $\delta \rightarrow 0$, gives

$$\bar{\alpha}^2 |\bar{\Omega}| = \lim_{\delta \rightarrow 0} \int_{\partial V_\delta} \frac{\partial \chi_{01}}{\partial n} ds = \int_{\partial\Omega} \frac{\partial \chi_{01}}{\partial n} ds + \sum_{j=1}^N \lim_{\delta \rightarrow 0} \int_{\partial B_\delta(\mathbf{X}_j(T))} \frac{\partial \chi_{01}}{\partial n} ds = -2\pi \sum_{j=1}^N C_{2j}, \tag{47}$$

where

$$|\bar{\Omega}| = \int_{\Omega} d\mathbf{X} = \epsilon^2 \int_{\Omega} dx = \epsilon^2 |\Omega|,$$

is the area of the domain in terms of the outer variable \mathbf{X} .

3.2 Inner region

The inner region is exactly the same as in §2.2.

3.3 Inner limit of the outer

The solution to (46) may be written as

$$\chi_{01} = 2\pi \sum_{j=1}^N C_{2j}(T) \bar{G}_n(\mathbf{X}; \mathbf{X}_j) + 2\pi \sum_{j=1}^N n_j \bar{H}(\mathbf{X}; \mathbf{X}_j) = \bar{\mathcal{G}},$$

say, where $\bar{G}_n(\mathbf{X}; \mathbf{Y})$ is the Neumann Green's function for Laplace's equation in Ω , satisfying

$$\nabla^2 \bar{G}_n = \delta(\mathbf{X} - \mathbf{Y}) - \frac{1}{|\bar{\Omega}|} \quad \text{in } \Omega, \quad \frac{\partial \bar{G}_n}{\partial n} = 0 \quad \text{on } \partial\Omega, \tag{48}$$

and \bar{H} satisfies

$$\nabla^2 \bar{H} = 0 \quad \text{in } \Omega \setminus \{\mathbf{Y}\}, \quad \frac{\partial \bar{H}}{\partial n} = 0 \quad \text{on } \partial\Omega, \quad \bar{H} \sim \frac{\phi}{2\pi} \text{ as } \mathbf{X} \rightarrow \mathbf{Y},$$

where ϕ is the azimuthal angle centred at \mathbf{Y} . If $\bar{G}_d(\mathbf{X}; \mathbf{Y})$ is the Dirichlet Green's function, satisfying

$$\nabla^2 \bar{G}_d = \delta(\mathbf{X} - \mathbf{Y}) \quad \text{in } \Omega, \quad \bar{G}_d = 0 \quad \text{on } \partial\Omega,$$

then \bar{H} is its harmonic conjugate, so that

$$\frac{\partial \bar{H}}{\partial x} = -\frac{\partial \bar{G}_d}{\partial y}, \quad \frac{\partial \bar{H}}{\partial y} = \frac{\partial \bar{G}_d}{\partial x}.$$

Defining the regular part of \overline{G}_n , \overline{H} and \overline{G}_d as

$$\begin{aligned}\overline{G}_n(\mathbf{X}; \mathbf{Y}) &= \frac{1}{2\pi} \log |\mathbf{X} - \mathbf{Y}| + \overline{G}_{n,\text{reg}}(\mathbf{X}; \mathbf{Y}), \\ \overline{H}(\mathbf{X}; \mathbf{Y}) &= \frac{\phi}{2\pi} + \overline{H}_{\text{reg}}(\mathbf{X}; \mathbf{Y}), \\ \overline{G}_d(\mathbf{X}; \mathbf{Y}) &= \frac{1}{2\pi} \log |\mathbf{X} - \mathbf{Y}| + \overline{G}_{d,\text{reg}}(\mathbf{X}; \mathbf{Y}),\end{aligned}$$

and

$$\begin{aligned}\overline{\mathcal{G}}_{\text{reg}}^\ell &= 2\pi C_{2\ell}(T) \overline{G}_{n,\text{reg}}(\mathbf{X}; \mathbf{X}_\ell) + 2\pi n_\ell \overline{H}_{\text{reg}}(\mathbf{X}; \mathbf{X}_\ell) \\ &\quad + 2\pi \sum_{j=1, j \neq \ell}^N C_{2j}(T) \overline{G}_n(\mathbf{X}; \mathbf{X}_j) + 2\pi \sum_{j=1, j \neq \ell}^N n_j \overline{H}(\mathbf{X}; \mathbf{X}_j),\end{aligned}\quad (49)$$

we find that as $\mathbf{X} \rightarrow \mathbf{X}_\ell(T)$,

$$\chi_0 \sim n_\ell \phi + C_{2\ell} \log |\mathbf{X} - \mathbf{X}_\ell(T)| + \overline{\mathcal{G}}_{\text{reg}}^\ell(\mathbf{X}_\ell) + (\mathbf{X} - \mathbf{X}_\ell(T)) \cdot \nabla \overline{\mathcal{G}}_{\text{reg}}^\ell(\mathbf{X}_\ell) + \dots \quad (50)$$

Written in terms of the inner variable $\epsilon \mathbf{x} = \mathbf{X} - \mathbf{X}_\ell(T)$ this is

$$\chi_0 \sim n_\ell \phi + C_{2\ell} \log(\epsilon r) + \overline{\mathcal{G}}_{\text{reg}}^\ell(\mathbf{X}_\ell) + \epsilon \mathbf{x} \cdot \nabla \overline{\mathcal{G}}_{\text{reg}}^\ell(\mathbf{X}_\ell) + \dots, \quad (51)$$

where r and ϕ are the polar representation of \mathbf{x} .

3.4 Outer limit of the inner

We sum the q -expansion of the outer limit of the inner in exactly the same way as in §2.4 to give $\widehat{\chi}_{00} = n_\ell \phi + (1/q) \log H_0$ with

$$H_0 = A_\ell(q) \epsilon^{-iqn_\ell} R^{iqn_\ell} + B_\ell(q) \epsilon^{iqn_\ell} R^{-iqn_\ell}.$$

To determine A_ℓ and B_ℓ we need to write $\widehat{\chi}_{00}$ in terms of r , expand in powers of q , and compare with (20). Crucially though, as mentioned in §3.1, and in contrast to §2.4, the expansions for A_ℓ and B_ℓ proceed now as $A_\ell(q) \sim A_{\ell 0} + qA_{\ell 1} + \dots$ and $B_\ell(q) \sim B_{\ell 0} + qB_{\ell 1} + \dots$. Expressing H_0 in terms of r we find

$$\begin{aligned}H_0(r) &\sim A_{\ell 0} + B_{\ell 0} + q(A_{\ell 1} + B_{\ell 1}) + q(A_{\ell 0} - B_{\ell 0}) i n_\ell \log r \\ &\quad + q^2 \left(A_{\ell 2} + B_{\ell 2} + (A_{\ell 1} - B_{\ell 1}) i n_k \log r - \frac{(A_{\ell 0} + B_{\ell 0})}{2} \log^2 r \right) + \dots,\end{aligned}\quad (52)$$

so that

$$\begin{aligned}\frac{\partial \widehat{\chi}_{00}}{\partial r} = \frac{H'_0(r)}{qH_0(r)} &\sim \frac{n_\ell(A_{\ell 0} - B_{\ell 0})i}{r(A_{\ell 0} + B_{\ell 0})} + q \left(\frac{(A_{\ell 1} - B_{\ell 1}) n_\ell i}{(A_{\ell 0} + B_{\ell 0}) r} - \frac{\log r}{r} \right. \\ &\quad \left. + \frac{(A_{\ell 0} - B_{\ell 0})^2 \log r}{(A_{\ell 0} + B_{\ell 0})^2 r} - \frac{i(A_{\ell 0} - B_{\ell 0})(A_{\ell 1} + B_{\ell 1}) n_\ell}{(A_{\ell 0} + B_{\ell 0})^2 r} \right) + \dots\end{aligned}$$

Comparing with (20) (and recalling that $n_\ell = \pm 1$) we see that

$$A_{\ell 0} - B_{\ell 0} = 0, \quad (53)$$

$$\frac{(A_{\ell 1} - B_{\ell 1})i}{A_{\ell 0} + B_{\ell 0}} = -n_\ell c_1 \quad \text{for } \ell = 1, \dots, N. \quad (54)$$

The remaining equations determining A_ℓ and B_ℓ will be fixed when matching with the outer region.

Using (53) we now find that (52) gives the outer limit of the leading-order inner expansion as

$$\begin{aligned} \widehat{\chi}_{00} &\sim \frac{1}{q} \log \left(A_{0\ell} (e^{-iqn_\ell \log \epsilon} + e^{iqn_\ell \log \epsilon}) \right) + n_\ell \phi + \frac{A_{1\ell} e^{-iqn_\ell \log \epsilon} + B_{1\ell} e^{iqn_\ell \log \epsilon}}{A_{0\ell} (e^{-iqn_\ell \log \epsilon} + e^{iqn_\ell \log \epsilon})} \\ &+ in \frac{(e^{-iqn_\ell \log \epsilon} - e^{iqn_\ell \log \epsilon})}{(e^{-iqn_\ell \log \epsilon} + e^{iqn_\ell \log \epsilon})} \log R + O(q). \end{aligned} \quad (55)$$

Similarly, the leading-order outer limit of the first correction to the inner expansion $\widehat{\chi}_{10}$ is, as before,

$$\widehat{\chi}_{10} \sim -\frac{\mu}{4q} \epsilon r \left(\frac{e^{-iqn_\ell \log \epsilon} (V_1 - iV_2) (1 + \gamma_1) e^{i\phi}}{e^{-iqn_\ell \log \epsilon} + e^{iqn_\ell \log \epsilon}} + \frac{e^{iqn_\ell \log \epsilon} (V_1 + iV_2) (1 + \gamma_2) e^{-i\phi}}{e^{-iqn_\ell \log \epsilon} + e^{iqn_\ell \log \epsilon}} \right).$$

3.5 Leading order matching: determination of the asymptotic wavenumber

Matching (51) with (55) gives

$$0 = \log \left(A_{0\ell} (e^{-iqn_\ell \log \epsilon} + e^{iqn_\ell \log \epsilon}) \right), \quad (56)$$

$$C_{2\ell} = in_\ell \frac{(e^{-iqn_\ell \log \epsilon} - e^{iqn_\ell \log \epsilon})}{(e^{-iqn_\ell \log \epsilon} + e^{iqn_\ell \log \epsilon})} = n_\ell \tan(qn_\ell \log \epsilon), \quad (57)$$

$$\overline{\mathcal{G}}_{\text{reg}}(\mathbf{X}_\ell) = \frac{A_{1\ell} e^{-iqn_\ell \log \epsilon} + B_{1\ell} e^{iqn_\ell \log \epsilon}}{A_{0\ell} (e^{-iqn_\ell \log \epsilon} + e^{iqn_\ell \log \epsilon})}. \quad (58)$$

Equation (56) gives $2A_{0\ell} = \text{cosec}(qn_\ell \log \epsilon)$. When $|n_j| = 1$ equation (57) implies the constants C_{2j} are all equal and given by

$$C_{2j} = -\tan(q \log(1/\epsilon)) \quad \forall j.$$

Equations (47) and (57) together determine $\bar{\alpha}$ via

$$\bar{\alpha}^2 = \frac{2\pi}{|\Omega|} \sum_{j=1}^N n_j \tan(qn_j \log(1/\epsilon)) = \frac{2\pi N}{|\Omega|} \tan(q \log(1/\epsilon)). \quad (59)$$

The asymptotic wavenumber is related to α by $k = \alpha\epsilon/q$ and so, since $\alpha = q^{1/2}\bar{\alpha}$,

$$k = \frac{\epsilon\bar{\alpha}}{q^{1/2}} = \frac{\epsilon}{q^{1/2}} \left(\frac{2\pi N}{|\Omega|} \tan(q \log(1/\epsilon)) \right)^{1/2} = \left(\frac{2\pi N}{q|\Omega|} \tan(q \log(1/\epsilon)) \right)^{1/2}. \quad (60)$$

As $q \log(1/\epsilon) \rightarrow \pi/2$ this expression matches smoothly into that given by (33); we demonstrate this in Section 4.3 when we develop a uniform composite approximation.

3.6 First order matching: law of motion for the spirals

Matching (51) with (34) gives

$$\begin{aligned} \mathbf{x} \cdot \nabla \overline{\mathcal{G}}_{\text{reg}}^\ell(\mathbf{X}_\ell) &\sim \left(\frac{4\gamma_1 - \tilde{\mu} A_{\ell 0} e^{-iqn_\ell \log \epsilon} (V_{1\ell} - iV_{2\ell})}{4(A_{\ell 0} e^{-iqn_\ell \log \epsilon} + B_{\ell 0} e^{iqn_\ell \log \epsilon})} \right) r e^{i\phi} \\ &+ \left(\frac{4\gamma_2 - \tilde{\mu} B_{\ell 0} e^{iqn_\ell \log \epsilon} (V_{1\ell} + iV_{2\ell})}{4(A_{\ell 0} e^{-iqn_\ell \log \epsilon} + B_{\ell 0} e^{iqn_\ell \log \epsilon})} \right) r e^{-i\phi}. \end{aligned}$$

Solving for γ_1 and γ_2 and substituting into (34) using (30) gives, finally,

$$\begin{aligned} \chi_{10} \sim & -\frac{\tilde{\mu}r}{4} (V_{1\ell} \cos \phi + V_{2\ell} \sin \phi) + \frac{\tilde{\mu}r}{4} (V_{1\ell} \cos(\phi - 2qn_\ell \log \epsilon) + V_{2\ell} \sin(\phi - 2qn_\ell \log \epsilon)) \\ & + r \cos(qn_\ell \log \epsilon) \left(\frac{\partial \bar{\mathcal{G}}_{\text{reg}}^\ell}{\partial X}(\mathbf{X}_\ell) \cos(\phi - qn_\ell \log \epsilon) + \frac{\partial \bar{\mathcal{G}}_{\text{reg}}^\ell}{\partial Y}(\mathbf{X}_\ell) \sin(\phi - qn_\ell \log \epsilon) \right) \end{aligned} \quad (61)$$

The compatibility condition (37) then gives the law of motion as

$$\frac{d\mathbf{X}_\ell}{dT} = \frac{2}{\tilde{\mu}} \cot(qn_\ell \log \epsilon) \nabla^\perp \bar{\mathcal{G}}_{\text{reg}}^\ell(\mathbf{X}_\ell). \quad (62)$$

Using (49) and (57) we may write this as

$$\begin{aligned} \frac{\tilde{\mu}}{2} \tan(qn_\ell \log \epsilon) \frac{d\mathbf{X}_\ell}{dT} &= 2\pi(n_\ell \tan(qn_\ell \log \epsilon)) \nabla^\perp \bar{\mathcal{G}}_{\text{n,reg}}(\mathbf{X}_\ell; \mathbf{X}_\ell) + 2\pi n_\ell \nabla^\perp \bar{\mathcal{H}}_{\text{reg}}(\mathbf{X}_\ell; \mathbf{X}_\ell) \\ &+ 2\pi \sum_{j=1, j \neq \ell}^N (n_j \tan(qn_j \log \epsilon)) \nabla^\perp \bar{\mathcal{G}}_{\text{n}}(\mathbf{X}_\ell; \mathbf{X}_j) \\ &+ 2\pi \sum_{j=1, j \neq \ell}^N n_j \nabla^\perp \bar{\mathcal{H}}(\mathbf{X}_\ell; \mathbf{X}_j) \\ &= 2\pi n_\ell \tan(qn_\ell \log \epsilon) \nabla^\perp \bar{\mathcal{G}}_{\text{n,reg}}(\mathbf{X}_\ell; \mathbf{X}_\ell) - 2\pi n_\ell \nabla \bar{\mathcal{G}}_{\text{d,reg}}(\mathbf{X}_\ell; \mathbf{X}_\ell) \\ &+ 2\pi \sum_{j=1, j \neq \ell}^N n_j \tan(qn_j \log \epsilon) \nabla^\perp \bar{\mathcal{G}}_{\text{n}}(\mathbf{X}_\ell; \mathbf{X}_j) \\ &- 2\pi \sum_{j=1, j \neq \ell}^N n_j \nabla \bar{\mathcal{G}}_{\text{d}}(\mathbf{X}_\ell; \mathbf{X}_j). \end{aligned} \quad (63)$$

Thus we see the motion due to each spiral is a mix of the gradient of the Dirichlet Green's function and the perpendicular gradient of the Neumann Green's function.

Since we are considering only the case that $|n_j| = 1$ for all j we may simplify to

$$\begin{aligned} n_\ell \frac{\mu}{2q} \tan(q \log \epsilon) \frac{d\mathbf{X}_\ell}{dT} &= 2\pi \tan(q \log \epsilon) \nabla^\perp \bar{\mathcal{G}}_{\text{n,reg}}(\mathbf{X}_\ell; \mathbf{X}_\ell) - 2\pi n_\ell \nabla \bar{\mathcal{G}}_{\text{d,reg}}(\mathbf{X}_\ell; \mathbf{X}_\ell) \\ &+ 2\pi \tan(q \log \epsilon) \sum_{j=1, j \neq \ell}^N \nabla^\perp \bar{\mathcal{G}}_{\text{n}}(\mathbf{X}_\ell; \mathbf{X}_j) \\ &- 2\pi \sum_{j=1, j \neq \ell}^N n_j \nabla \bar{\mathcal{G}}_{\text{d}}(\mathbf{X}_\ell; \mathbf{X}_j) \end{aligned} \quad (64)$$

As the size of the domain tends to infinity both the Neumann and Dirichlet Green's functions tend to

$$\frac{1}{2\pi} \log |\mathbf{X} - \mathbf{Y}|.$$

Equation (63) then becomes

$$\frac{\tilde{\mu}}{2} \tan(qn_\ell \log \epsilon) \frac{d\mathbf{X}_\ell}{dT} = \sum_{j=1, j \neq \ell}^N \frac{n_j \tan(qn_j \log \epsilon)}{|\mathbf{X}_\ell - \mathbf{X}_j|} \mathbf{e}_{\phi_j} + \sum_{j=1, j \neq \ell}^N \frac{n_j}{|\mathbf{X}_\ell - \mathbf{X}_j|} \mathbf{e}_{r_j}$$

in agreement with [2].

4 Comparison with direct numerical simulations

In this section we compare our results with direct numerical simulations in a rectangular domain with sides of length a and b . As we have shown in the previous sections, we find two different laws of motion for spirals depending on the relative sizes of the domain and the parameter q . We first evaluate these two laws of motion for the case of a rectangle, before comparing the trajectories and velocity of spirals with those obtained by numerically solving the partial differential equation (5).

4.1 Canonical scale

For spirals in a rectangular domains in which $a, b \sim 1/\epsilon \sim e^{\pi/2q}$ the motion takes place in the canonical scaling. Recalling that the outer variable is defined as $\mathbf{X} = \epsilon \mathbf{x}$, equation (13) for the Neumann Green's function $G(\mathbf{X}; \hat{\mathbf{X}})$ for the modified Helmholtz equation is, in this case

$$\begin{aligned} \nabla^2 G - \alpha^2 G &= \delta(\mathbf{X} - \hat{\mathbf{X}}) \quad \text{in } [0, \epsilon a] \times [0, \epsilon b], \\ \frac{\partial G}{\partial X} &= 0 \quad \text{on } X = 0 \text{ and } X = \epsilon a, \\ \frac{\partial G}{\partial Y} &= 0 \quad \text{on } Y = 0 \text{ and } Y = \epsilon b, \end{aligned}$$

where $\mathbf{X} = (X, Y)$ and $\hat{\mathbf{X}} = (\hat{X}, \hat{Y})$. Using the method of images, and noting that the free space Green's function is given by (41), the solution is

$$\begin{aligned} G(\mathbf{X}; \hat{\mathbf{X}}) &= -\frac{1}{2\pi} \sum_{m,n=-\infty}^{\infty} K_0 \left(\alpha \left((X - \hat{X} + 2n\epsilon a)^2 + (Y - \hat{Y} + 2m\epsilon b)^2 \right)^{1/2} \right) \\ &\quad - \frac{1}{2\pi} \sum_{m,n=-\infty}^{\infty} K_0 \left(\alpha \left((X + \hat{X} + 2n\epsilon a)^2 + (Y - \hat{Y} + 2m\epsilon b)^2 \right)^{1/2} \right) \\ &\quad - \frac{1}{2\pi} \sum_{m,n=-\infty}^{\infty} K_0 \left(\alpha \left((X - \hat{X} + 2n\epsilon a)^2 + (Y + \hat{Y} + 2m\epsilon b)^2 \right)^{1/2} \right) \\ &\quad - \frac{1}{2\pi} \sum_{m,n=-\infty}^{\infty} K_0 \left(\alpha \left((X + \hat{X} + 2n\epsilon a)^2 + (Y + \hat{Y} + 2m\epsilon b)^2 \right)^{1/2} \right). \end{aligned}$$

The series are rapidly convergent since $K_0(z)$ decays exponentially for large z . We also defined the regular part of the Green's function by

$$G_{\text{reg}}(\mathbf{X}; \hat{\mathbf{X}}) = G(\mathbf{X}; \hat{\mathbf{X}}) - \frac{1}{2\pi} \log |\mathbf{X} - \hat{\mathbf{X}}|.$$

In order to compare with direct numerical simulation, we rewrite G in terms of the original variable \mathbf{x} by setting

$$\begin{aligned}
G'(\mathbf{x}; \boldsymbol{\xi}) = G(\epsilon\mathbf{x}; \epsilon\boldsymbol{\xi}) &= -\frac{1}{2\pi} \sum_{m,n=-\infty}^{\infty} K_0 \left(qk \left((x - \xi + 2na)^2 + (y - \eta + 2mb)^2 \right)^{1/2} \right) \\
&\quad - \frac{1}{2\pi} \sum_{m,n=-\infty}^{\infty} K_0 \left(qk \left((x + \xi + 2na)^2 + (y - \eta + 2mb)^2 \right)^{1/2} \right) \\
&\quad - \frac{1}{2\pi} \sum_{m,n=-\infty}^{\infty} K_0 \left(qk \left((x - \xi + 2na)^2 + (y + \eta + 2mb)^2 \right)^{1/2} \right) \\
&\quad - \frac{1}{2\pi} \sum_{m,n=-\infty}^{\infty} K_0 \left(qk \left((x + \xi + 2na)^2 + (y + \eta + 2mb)^2 \right)^{1/2} \right),
\end{aligned}$$

where $\hat{\mathbf{X}} = \epsilon\boldsymbol{\xi} = \epsilon(\xi, \eta)$, and we have written $\epsilon\alpha = qk$. Then

$$G'_{\text{reg}}(\mathbf{x}; \boldsymbol{\xi}) = G'(\mathbf{x}; \boldsymbol{\xi}) - \frac{1}{2\pi} \log |\mathbf{x} - \boldsymbol{\xi}| = G_{\text{reg}}(\epsilon\mathbf{x}; \epsilon\boldsymbol{\xi}) + \frac{1}{2\pi} \log \epsilon.$$

With a single spiral. In the particular case where there is only one spiral at position \mathbf{X}_1 with unitary winding number n_1 , the law of motion simply reads

$$\frac{d\mathbf{X}_1}{dT} = \frac{4\pi q n_1}{\mu} \nabla^\perp G_{\text{reg}}(\mathbf{X}_1; \mathbf{X}_1), \quad (65)$$

and α is given by

$$-2\pi G_{\text{reg}}(\mathbf{X}_1; \mathbf{X}_1) + c_1 + \log(1/\epsilon) - \pi/2q = 0. \quad (66)$$

Written in terms of the original variables \mathbf{x} , t and k equation (65) becomes

$$\frac{d\mathbf{x}_1}{dt} = 4\pi q n_1 \nabla^\perp G'_{\text{reg}}(\mathbf{x}_1; \mathbf{x}_1) \quad (67)$$

where ∇ now represents the gradient with respect to \mathbf{x} . Equation (66) becomes

$$-2\pi G'_{\text{reg}}(\mathbf{x}_1; \mathbf{x}_1) + c_1 - \pi/2q = 0.$$

Note that neither of these equations depends on the scaling parameters ϵ or μ , as expected.

With two spirals Written in terms of the original coordinate \mathbf{x} , with spirals at positions \mathbf{x}_1 and \mathbf{x}_2 , (39) gives

$$\begin{aligned}
2\pi\beta_1 G'_{\text{reg}}(\mathbf{x}_1; \mathbf{x}_1) + 2\pi\beta_2 G'(\mathbf{x}_1; \mathbf{x}_2) - \beta_1(c_1 - \pi/2q) &= 0, \\
2\pi\beta_2 G'_{\text{reg}}(\mathbf{x}_2; \mathbf{x}_2) + 2\pi\beta_1 G'(\mathbf{x}_2; \mathbf{x}_1) - \beta_2(c_1 - \pi/2q) &= 0.
\end{aligned}$$

The equation for k is thus

$$(-2\pi G'_{\text{reg}}(\mathbf{x}_1; \mathbf{x}_1) + c_1 - \pi/2q) (-2\pi G'_{\text{reg}}(\mathbf{x}_2; \mathbf{x}_2) + c_1 - \pi/2q) = 4\pi^2 G'(\mathbf{x}_2; \mathbf{x}_1) G'(\mathbf{x}_1; \mathbf{x}_2),$$

while

$$\frac{\beta_2}{\beta_1} = \frac{2\pi G'_{\text{reg}}(\mathbf{x}_1; \mathbf{x}_1) - c_1 + \pi/2q}{2\pi G'(\mathbf{x}_1; \mathbf{x}_2)} = \frac{2\pi G'(\mathbf{x}_2; \mathbf{x}_1)}{2\pi G'_{\text{reg}}(\mathbf{x}_2; \mathbf{x}_2) - c_1 + \pi/2q}.$$

Note that $G'(\mathbf{x}_2; \mathbf{x}_1) = G'(\mathbf{x}_1; \mathbf{x}_2)$.

Written in terms of the original variables \mathbf{x} and t the law of motion (65) for two spirals is

$$\begin{aligned}\frac{d\mathbf{x}_1}{dt} &= 4\pi q n_1 \frac{\beta_2}{\beta_1} \nabla^\perp G'(\mathbf{x}_1; \mathbf{x}_2) + 4\pi q n_1 \nabla^\perp G'_{\text{reg}}(\mathbf{x}_1; \mathbf{x}_1) \\ \frac{d\mathbf{x}_2}{dt} &= 4\pi q n_2 \frac{\beta_1}{\beta_2} \nabla^\perp G'(\mathbf{x}_2; \mathbf{x}_1) + 4\pi q n_2 \nabla^\perp G'_{\text{reg}}(\mathbf{x}_2; \mathbf{x}_2).\end{aligned}$$

Remark 1 We note that if initially $\mathbf{x}_1 + \mathbf{x}_2 = (a, b)$, so that the spirals are placed symmetrically with respect to the centre of the domain, then if $n_1 = n_2$ they keep this symmetry during the motion. In this case $G'_{\text{reg}}(\mathbf{x}_1; \mathbf{x}_1) = G'_{\text{reg}}(\mathbf{x}_2; \mathbf{x}_2)$ so that $\beta_2/\beta_1 = 1$.

4.2 Near-field scale

In the near field scaling the relevant Green's functions are the Neumann and Dirichlet Green's functions for Laplace's equation. We rewrite these in the original variables as $G'_n(\mathbf{x}; \boldsymbol{\xi}) = \overline{G}_n(\epsilon\mathbf{x}; \epsilon\boldsymbol{\xi})$, $G'_d(\mathbf{x}; \boldsymbol{\xi}) = \overline{G}_d(\epsilon\mathbf{x}; \epsilon\boldsymbol{\xi})$. As before, we evaluate the Green's functions by the method of images. However, we must be a little careful, because the sums over images for the Green's functions themselves do not converge. However, the corresponding sums over images for the derivatives of the Green's functions do converge, and these are what we need for the law of motion. Defining

$$\begin{aligned}V_x(\mathbf{x}; \xi, \eta) &= \frac{1}{2\pi} \sum_{n,m=-\infty}^{\infty} \frac{x - \xi + 2an}{(x - \xi + 2na)^2 + (y - \eta + 2mb)^2} \\ &= \frac{1}{2\pi} \sum_{m=-\infty}^{\infty} \frac{\pi \sin(\pi(x - \xi)/a)}{2a(\cosh(\pi((y - \eta) + 2bm)/a) - \cos(\pi(x - \xi)/a))}, \\ V_y(\mathbf{x}; \xi, \eta) &= \frac{1}{2\pi} \sum_{n,m=-\infty}^{\infty} \frac{y - \eta + 2bm}{(x - \xi + 2na)^2 + (y - \eta + 2mb)^2} \\ &= \frac{1}{2\pi} \sum_{n=-\infty}^{\infty} \frac{\pi \sin(\pi(y - \eta)/b)}{2b(\cosh(\pi((x - \xi) + 2an)/b) - \cos(\pi(y - \eta)/b))},\end{aligned}$$

then

$$\begin{aligned}\frac{\partial G'_n}{\partial x}(\mathbf{x}; \boldsymbol{\xi}) &= V_x(\mathbf{x}; \xi, \eta) + V_x(\mathbf{x}; -\xi, \eta) + V_x(\mathbf{x}; \xi, -\eta) + V_x(\mathbf{x}; -\xi, -\eta), \\ \frac{\partial G'_n}{\partial y}(\mathbf{x}; \boldsymbol{\xi}) &= V_y(\mathbf{x}; \xi, \eta) + V_y(\mathbf{x}; -\xi, \eta) + V_y(\mathbf{x}; \xi, -\eta) + V_y(\mathbf{x}; -\xi, -\eta), \\ \frac{\partial G'_d}{\partial x}(\mathbf{x}; \boldsymbol{\xi}) &= V_x(\mathbf{x}; \xi, \eta) - V_x(\mathbf{x}; -\xi, \eta) - V_x(\mathbf{x}; \xi, -\eta) + V_x(\mathbf{x}; -\xi, -\eta), \\ \frac{\partial G'_d}{\partial y}(\mathbf{x}; \boldsymbol{\xi}) &= V_y(\mathbf{x}; \xi, \eta) - V_y(\mathbf{x}; -\xi, \eta) - V_y(\mathbf{x}; \xi, -\eta) + V_y(\mathbf{x}; -\xi, -\eta).\end{aligned}$$

Note that the final sums above again converge exponentially quickly. In terms of \mathbf{x} and t the law of motion is

$$\begin{aligned}\frac{n_\ell}{2q} \tan(q \log \epsilon) \frac{d\mathbf{x}_\ell}{dt} &= 2\pi \tan(q \log \epsilon) \nabla^\perp G'_{n,\text{reg}}(\mathbf{x}_\ell; \mathbf{x}_\ell) - 2\pi n_\ell \nabla G'_{d,\text{reg}}(\mathbf{x}_\ell; \mathbf{x}_\ell) \\ &\quad + 2\pi \tan(q \log \epsilon) \sum_{j=1, j \neq \ell}^N \nabla^\perp G'_n(\mathbf{x}_\ell; \mathbf{x}_j) - 2\pi \sum_{j=1, j \neq \ell}^N n_j \nabla G'_d(\mathbf{x}_\ell; \mathbf{x}_j).\end{aligned}$$

Recall also that

$$k = \left(\frac{2\pi N}{q|\Omega|} \tan(q \log(1/\epsilon)) \right)^{1/2},$$

where $|\Omega|$ is the area of Ω in the original variable \mathbf{x} .

With a single spiral Written out in component form, the law of motion for a single spiral at \mathbf{x}_1 with winding number $|n_1| = 1$ is

$$\begin{aligned} \frac{dx_1}{dt} &= -4\pi q n_1 \frac{\partial G'_{n,\text{reg}}(\mathbf{x}_1; \mathbf{x}_1)}{\partial y} - 4\pi q \cot(q \log \epsilon) \frac{\partial G'_{d,\text{reg}}(\mathbf{x}_1; \mathbf{x}_1)}{\partial x}, \\ \frac{dy_1}{dt} &= 4\pi q n_1 \frac{\partial G'_{n,\text{reg}}(\mathbf{x}_1; \mathbf{x}_1)}{\partial x} - 4\pi q \cot(q \log \epsilon) \frac{\partial G'_{d,\text{reg}}(\mathbf{x}_1; \mathbf{x}_1)}{\partial y}. \end{aligned}$$

With two spirals Written out in component form, the law of motion for spirals at positions \mathbf{x}_1 and \mathbf{x}_2 with winding numbers $|n_1| = |n_2| = 1$ is

$$\begin{aligned} \frac{dx_1}{dt} &= -4\pi q n_1 \frac{\partial G'_{n,\text{reg}}(\mathbf{x}_1; \mathbf{x}_1)}{\partial y} - 4\pi q \cot(q \log \epsilon) \frac{\partial G'_{d,\text{reg}}(\mathbf{x}_1; \mathbf{x}_1)}{\partial x} \\ &\quad - 4\pi q n_1 \frac{\partial G'_n(\mathbf{x}_1; \mathbf{x}_2)}{\partial y} - 4\pi q n_2 n_1 \cot(q \log \epsilon) \frac{\partial G'_d(\mathbf{x}_1; \mathbf{x}_2)}{\partial x}, \\ \frac{dy_1}{dt} &= 4\pi q n_1 \frac{\partial G'_{n,\text{reg}}(\mathbf{x}_1; \mathbf{x}_1)}{\partial x} - 4\pi q \cot(q \log \epsilon) \frac{\partial G'_{d,\text{reg}}(\mathbf{x}_1; \mathbf{x}_1)}{\partial y} \\ &\quad + 4\pi n_1 q \frac{\partial G'_n(\mathbf{x}_1; \mathbf{x}_2)}{\partial x} - 4\pi q n_1 n_2 \cot(q \log \epsilon) \frac{\partial G'_d(\mathbf{x}_1; \mathbf{x}_2)}{\partial y}, \\ \frac{dx_2}{dt} &= -4\pi n_2 q \frac{\partial G'_{n,\text{reg}}(\mathbf{x}_2; \mathbf{x}_2)}{\partial y} - 4\pi q \cot(q \log \epsilon) \frac{\partial G'_{d,\text{reg}}(\mathbf{x}_2; \mathbf{x}_2)}{\partial x} \\ &\quad - 4\pi q n_2 \frac{\partial G'_n(\mathbf{x}_2; \mathbf{x}_1)}{\partial y} - 4\pi q n_1 n_2 \cot(q \log \epsilon) \frac{\partial G'_d(\mathbf{x}_2; \mathbf{x}_1)}{\partial x}, \\ \frac{dy_2}{dt} &= 4\pi q n_2 \frac{\partial G'_{n,\text{reg}}(\mathbf{x}_2; \mathbf{x}_2)}{\partial x} - 4\pi q \cot(q \log \epsilon) \frac{\partial G'_{d,\text{reg}}(\mathbf{x}_2; \mathbf{x}_2)}{\partial y} \\ &\quad + 4\pi q n_2 \frac{\partial G'_n(\mathbf{x}_2; \mathbf{x}_1)}{\partial x} - 4\pi q n_1 n_2 \cot(q \log \epsilon) \frac{\partial G'_d(\mathbf{x}_2; \mathbf{x}_1)}{\partial y}. \end{aligned}$$

4.3 A composite expansion

To compare with direct numerical simulations we combine the expansions of Sections 4.1 and 4.2 into a single composite expansion valid in both regions. We first consider the asymptotic wavenumber. As $\alpha \rightarrow 0$ in (13) we find

$$G(\mathbf{X}; \mathbf{Y}) \sim \frac{1}{|\Omega|\alpha^2} + \overline{G}_n(\mathbf{X}; \mathbf{Y}) + \dots,$$

where $\overline{G}_n(\mathbf{X}; \mathbf{Y})$ is the Neumann Greens function for Laplace's equation given by (48). Thus (33) implies that the β_ℓ are all equal to leading order and α is given by

$$\alpha^2 \sim \frac{2\pi N q}{|\Omega|(\pi/2 - q \log \epsilon)}.$$

We see that this matches smoothly into the near-field α we found in (59), since

$$\alpha^2 = q\bar{\alpha}^2 = \frac{2\pi qN}{|\bar{\Omega}|} \tan(q \log(1/\epsilon)) \sim \frac{2\pi Nq}{|\bar{\Omega}|(\pi/2 - q|\log \epsilon|)}$$

as $q|\log \epsilon| \rightarrow \pi/2$. We may generate a uniform approximation to α by taking

$$\alpha^2 = \alpha_{\text{canonical}}^2 + \alpha_{\text{near}}^2 - \frac{2\pi Nq}{|\bar{\Omega}|(\pi/2 - q|\log \epsilon|)}.$$

The corresponding uniform approximation to k is given by

$$k^2 = k_{\text{canonical}}^2 + \frac{2\pi N}{q|\bar{\Omega}|} \tan(q \log(1/\epsilon)) - \frac{2\pi N}{q|\bar{\Omega}|(\pi/2 - q|\log \epsilon|)}.$$

For the law of motion the simplest composite expansion is to use the near-field law of motion (64) but with the Neumann and Dirichlet Green's functions for the modified Helmholtz equation (13) in place of those for Laplace's equation.

In order to validate our results, numerical simulations of (1) were carried out using finite difference schemes applied to the coupled reaction-diffusion equations for the real and imaginary parts of ψ . The choice of the second-order accurate uniform spatial discretization follows other studies of spiral wave dynamics [8, 5]. Explicit timestepping using Euler's method with a small timestep, $\Delta t = \Delta x^2/20$, was found to be stable and computationally efficient. Trajectories of the spiral cores were obtained by tracking the minima of $|\psi|$. Initial conditions were chosen to have zeros with a unit winding number at the desired initial location of the spirals. Following initial transients, the numerical solutions converged locally to stable spiral-wave structures, maintained for long times. Because of this transient we might expect a small change in the initial position when comparing spiral trajectories with the solution of the asymptotic law of motion.

In order to plot the composite solution we need to make one final choice as to the value of ϵ , which is the inverse of the typical separation between spirals (and their images). In principle there should be no choice in this parameter (note that ϵ disappears from the approximation for k , for example, when it is rewritten in the original variables)—this is reflected in the law of motion by the fact that ϵ only appears as $\log(\epsilon)$: multiplying ϵ by any factor does not change the law of motion asymptotically. However, for finite values of q the choice of ϵ is important. The simplest choice would simply be the inverse of the domain diameter, i.e. $\epsilon = 1/a$. However, we find that a better match with the direct numerical simulations is achieved if ϵ is taken to be proportional to the inverse distance to the nearest image. For a single spiral we approximate this by setting

$$\epsilon = \lambda \left(\frac{1}{x_1^p} + \frac{1}{(a-x_1)^p} + \frac{1}{y_1^p} + \frac{1}{(b-y_1)^p} \right)^{1/p}, \quad (68)$$

where we take p to be 1, 2 or 3 and λ is an $O(1)$ constant chosen to give a good fit.

For two spirals we take

$$\epsilon = \lambda \left(\frac{1}{x_1^p} + \frac{1}{(a-x_1)^p} + \frac{1}{y_1^p} + \frac{1}{(b-y_1)^p} + \frac{1}{((a/2-x_1)^2 + (b/2-y_1)^2)^{p/2}} \right)^{1/p}, \quad (69)$$

and the results are fairly insensitive to p so we take $p = 1$ and $\lambda = 0.52$ for all q .

In Figure 1 we compare the trajectories provided by a direct numerical simulation of (1) (dashed lines) and those given by the uniform asymptotic approximation described above (solid lines) for a single spiral in a square domain of side 200. Numerical trajectories starting from

positions $(10, 0), (20, 0), \dots, (70, 0)$ are shown. The starting points for the asymptotic trajectories are perturbed slightly to account for the initial transient in the numerical simulation. These were determined by solving backwards from a point on the numerical trajectory near the boundary of the domain. While the qualitative behaviour of the trajectories is the same whatever value for ϵ is chosen (since the law of motion depends only on $\log \epsilon$ as we have noted), the excellent quantitative agreement shown relies on a careful choice of the parameters in (68).

For small q we see that the spiral is attracted to the boundary whatever its initial position. However, as q is increased there is a Hopf bifurcation with the appearance of an unstable periodic orbit. Trajectories starting outside this periodic orbit are attracted to the boundary of the domain, but those starting inside it spiral in to the origin. As q is increased further the periodic orbit grows in size and becomes more square. This can be understood as the spiral interacting with its images predominantly in the near-field limit, in which the motion is perpendicular to the line of centres. With the motion dominated by the nearest image the spiral will move parallel to the nearest boundary until it nears the corner, when a second image takes over.

In Figure 2 we compare the trajectories provided by a direct numerical simulation of (1) (dashed lines) and those given by the uniform asymptotic approximation (solid lines) for a pair of $+1$ spirals in the same square domain of side 200. We position the spirals symmetrically at positions $(-x, 0)$ and $(x, 0)$, where we choose $x = 10, 20, \dots, 70$. In this case we use the expression (69) for ϵ with $p = 1$ and $\lambda = 0.52$ for all q . As in Figure 1, the starting points of the asymptotic trajectories are perturbed to account for the initial transient in the numerical simulation, and were determined by solving backwards from a point on the numerical trajectory near the boundary of the domain.

We see that the agreement is qualitatively very good, but is less quantitative than in the single spiral case. An examination of the numerical trajectories indicates that there must be a stronger initial transient in this case. For example, in Figure 2(a) the numerical trajectories from initial positions $(50, 0)$ and $(60, 0)$ practically overlap at late times, and in fact cross each other. Since the asymptotic law of motion gives velocity as a function of position, such behaviour is not possible when the evolution is quasistatic.

In the trajectories of Figure 2 we see that the spirals attempt to circle around each other, as the near-field interaction would indicate, but gradually drift apart until the image spirals take over and force the pair to rotate in the opposite direction.

5 Conclusions

We have developed a law of motion for interacting spiral waves in a bounded domain in the limit that the twist parameter q is small. We find that the size of the domain is crucial in determining the form of this law of motion.

When the domain is large (specifically when the diameter is $O(e^{\pi/2q})$) the motion is given in terms of the Neumann Green's function for the modified Helmholtz equation (40). The asymptotic wavenumber, which is exponentially small in q , is determined as the solvability condition on a set of linear equations involving the positions of all the spirals (39).

When the domain is not so large, the motion is given in terms of both the Neumann and Dirichlet Green's functions for Laplace's equation (64). The asymptotic wavenumber is now algebraically small in q , and depends only on the number of spirals and not their position (60).

Although we have focussed on Neumann boundary conditions for the complex Ginzburg-Landau equation (4), the extension to periodic boundary conditions is straightforward.

Acknowledgements M. aguareles is part of the Catalan Research group 2017 SGR 1392 and has been supported by the MINECO grant MTM2017-84214-C2-2-P (Spain). The authors would also like to thank the centre OCIAM where part of this research was carried out.

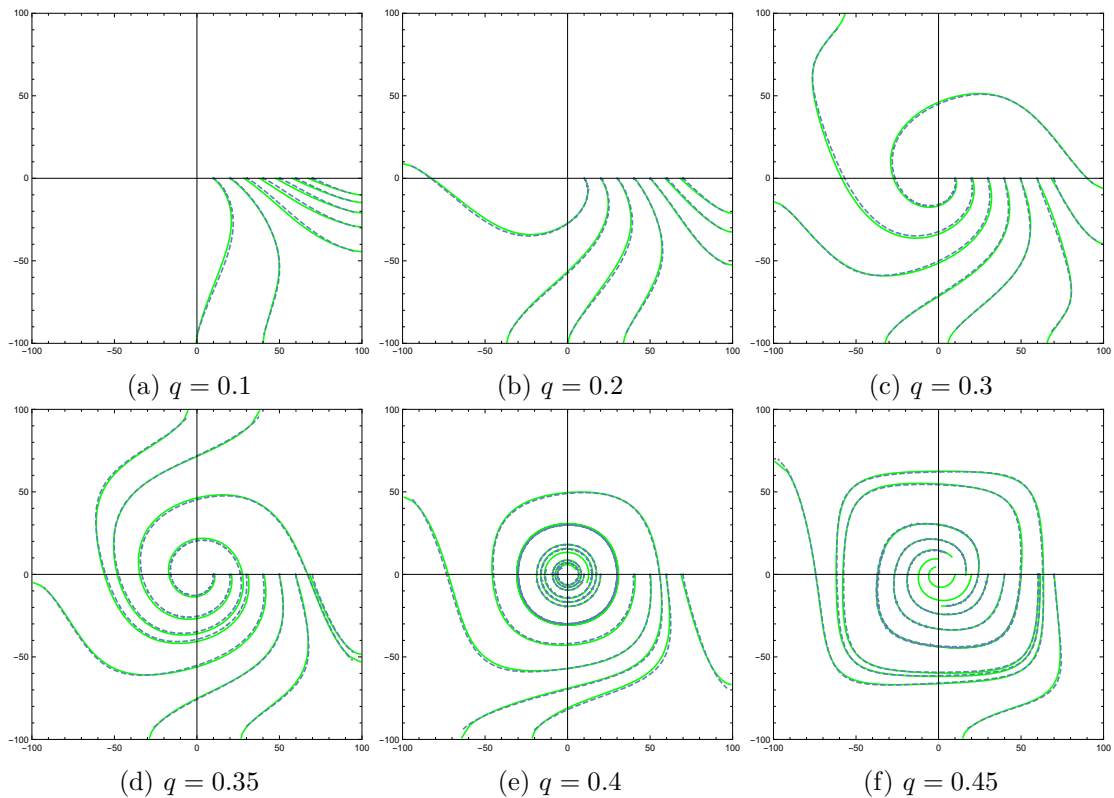


Figure 1: Comparison between the trajectories provided by a direct numerical simulation of (1) (dashed lines) and the uniform asymptotic approximation of §4.3 (solid lines) for a single spiral in a square domain of side 200. Numerical trajectories starting from positions $(10, 0), (20, 0), \dots, (70, 0)$ are shown; ϵ is given by (68) with (a) $p = 1, \lambda = 0.57$; (b) $p = 1, \lambda = 0.6$; (c) $p = 1, \lambda = 0.6$; (d) $p = 2, \lambda = 1.01$; (e) $p = 3, \lambda = 1.12$; (f) $p = 2, \lambda = 1$. The asymptotic starting points are perturbed slightly to account for the initial transient in the numerical simulation. Note the appearance of an unstable periodic orbit in (e) and (f) which is captured by the asymptotic law of motion. An extra orbit starting from position $(61, 0)$ is shown in (f)—the periodic orbit crosses the x -axis somewhere between 60 and 61.

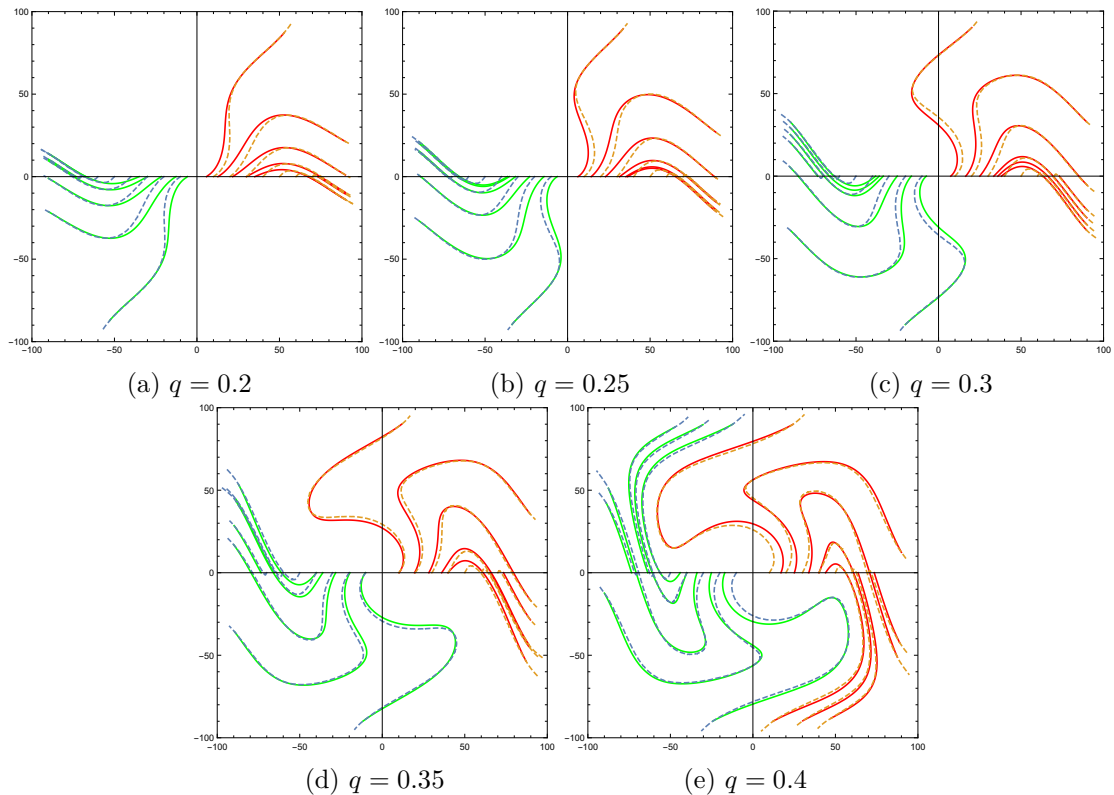


Figure 2: Comparison between the trajectories provided by a direct numerical simulation of (1) (dashed lines) and the uniform asymptotic approximation of §4.3 (solid lines) for a pair of spirals in a square domain of side 200. Spirals are placed symmetrically at positions $(-x, 0)$ and $(x, 0)$ with $x = 10, 20, \dots, 70$; ϵ is given by (69) with $p = 1$, $\lambda = 0.52$. The asymptotic starting points are perturbed to account for the initial transient in the numerical simulation.

References

- [1] M. Aguareles. The effect of boundaries on the asymptotic wavenumber of spiral wave solutions of the complex ginzburg–landau equation. *Physica D: Nonlinear Phenomena*, 278:1–12, 2014.
- [2] M. Aguareles, S. J. Chapman, and T. Witelski. Interaction of Spiral Waves in the Complex Ginzburg-Landau Equation. *Physical Review Letters*, 101(22), Nov 28 2008.
- [3] M. Aguareles, S. J. Chapman, and T. Witelski. Motion of spiral waves in the complex Ginzburg-Landau equation. *Phys. D*, 239(7):348–365, 2010.
- [4] Igor S. Aranson and Lorenz Kramer. The world of the complex Ginzburg-Landau equation. *Rev. Mod. Phys.*, 74(1):99–143, 2002.
- [5] M. Barkley, M. Kness, and L.S. Tukerman. Spiral-wave dynamics in a simple model of excitable media: the transition from simple to compound rotation. *Phys. Rev. A*, 42(4):2489–2492, 1990.
- [6] Tomas Bohr, Greg Huber, and Edward Ott. The structure of spiral-domain patterns and shocks in the 2D complex Ginzburg-Landau equation. *Phys. D*, 106(1-2):95–112, 1997.
- [7] Subir K Das. Unlocking of frozen dynamics in the complex ginzburg-landau equation. *Physical Review E*, 87(1):012135, 2013.
- [8] M. Dowle, R. M. Mantel, and D. Barkley. Fast simulations of waves in three-dimensional excitable media. *Int. J. of Bif. and Chaos*, 7(11):2529–2545, 1997.
- [9] Milton Van Dyke. *Perturbation methods in fluid mechanics*. Academic Press, New York, 1964. by Milton Van Dyke; il.;24 cm; Bibliografia; Applied mathematics and mechanics ;8.
- [10] Patrick S. Hagan. Spiral waves in reaction-diffusion equations. *SIAM J. Appl. Math.*, 42(4):762–786, 1982.
- [11] PC Hohenberg and AP Krekhov. An introduction to the ginzburg–landau theory of phase transitions and nonequilibrium patterns. *Physics Reports*, 572:1–42, 2015.
- [12] Y. Kuramoto. *Chemical oscillations, waves and turbulence*, volume 19 of *Springer Series in Synergetics*. Springer-Verlag, Berlin, 1984.
- [13] Jerome V. Moloney and Alan C. Newell. Nonlinear optics. *Phys. D*, 44(1-2):1–37, 1990.
- [14] Shahir Mowlaei, Ahmed Roman, and Michel Pleimling. Spirals and coarsening patterns in the competition of many species: a complex ginzburg–landau approach. *Journal of Physics A: Mathematical and Theoretical*, 47(16):165001, 2014.
- [15] L.N. Howard N. Kopell. Target pattern and spiral solutions to reaction. *Advances in Applied Mathematics*, 2:417–449, 1981.
- [16] John C. Neu. Vortices in complex scalar fields. *Phys. D*, 43(2-3):385–406, 1990.
- [17] Joseph Paultet, Bard Ermentrout, and William Troy. The existence of spiral waves in an oscillatory reaction-diffusion system. *SIAM J. Appl. Math.*, 54(5):1386–1401, 1994.
- [18] L. M. Pismen. Weakly radiative spiral waves. *Phys. D*, 184(1-4):141–152, 2003. Complexity and nonlinearity in physical systems (Tucson, AZ, 2001).

- [19] R. W. Walden, Paul Kolodner, A. Passner, and C. M. Surko. Traveling waves and chaos in convection in binary fluid mixtures. *Phys. Rev. Lett.*, 55(5):496–499, Jul 1985.
- [20] AN Zaikin and AM Zhabotinsky. Concentration wave propagation in two-dimensional liquid-phase self-oscillating system. *Nature*, 225(5232):535–537, 1970.